

## Probing the supersymmetric type III seesaw: LFV at low-energies and at the LHC

A. Abada<sup>a</sup>, A. J. R. Figueiredo<sup>b</sup>, J. C. Romão<sup>b</sup> and A. M. Teixeira<sup>c</sup>

<sup>a</sup> Laboratoire de Physique Théorique, CNRS – UMR 8627,  
Université de Paris-Sud 1, F-91405 Orsay Cedex, France

<sup>b</sup> Centro de Física Teórica de Partículas, Instituto Superior Técnico,  
Av. Rovisco Pais 1, 1049-001 Lisboa, Portugal

<sup>c</sup> Laboratoire de Physique Corpusculaire, CNRS/IN2P3 – UMR 6533,  
Campus des Cézeaux, 24 Av. des Landais, F-63171 Aubière Cedex, France

### Abstract

We consider a supersymmetric type III seesaw, where the additional heavy states are embedded into complete  $SU(5)$  representations to preserve gauge coupling unification. Complying with phenomenological and experimental constraints strongly tightens the viable parameter space of the model. In particular, one expects very characteristic signals of lepton flavour violation both at low-energies and at the LHC, which offer the possibility of falsifying the model.

KEYWORDS: Supersymmetry, LHC, slepton mass splittings, lepton flavour violation, seesaw mechanism

# 1 Introduction

The seesaw mechanism, in its different realisations, constitutes one of the simplest and yet most elegant ways to explain neutrino masses and mixings. In the minimal realisations of the seesaw, the Standard Model (SM) can be extended by the addition of fermionic singlets (type I seesaw) [1], scalar triplets (type II) [2] or fermionic triplets (type III) [3]. Although dependent on the size of the neutrino Yukawa couplings ( $Y^\nu$ ), these new states are in general heavy: assuming natural couplings,  $Y^\nu \sim 1$ , their masses can be close to the Grand Unified Theory (GUT) scale,  $\mathcal{O}(10^{16} \text{ GeV})$ .

If these states are indeed at the origin of neutrino mass generation, it is important to investigate which seesaw realisation (or combination thereof) is at work. Indeed, if the mass of the mediators is such that production at present colliders is possible (in this case  $Y^\nu \sim 10^{-6}$ ), then one can devise strategies for their direct searches. On the contrary, if they are very heavy, then they cannot be directly probed, and their indirect signatures in low-energy observables (typically via higher order corrections) will be extremely suppressed.

Other than the mechanism of neutrino mass generation, there are several reasons - theoretical issues and observational problems - motivating the extension (or embedding) of the SM into a larger framework. Supersymmetry (SUSY) is a well motivated solution for the hierarchy problem that also offers an elegant solution for the non-baryonic dark matter (DM) problem of the Universe [4–6]. If the Large Hadron Collider (LHC) indeed finds signatures of SUSY, it is then extremely appealing to consider the embedding of a seesaw mechanism into a supersymmetric framework (the so-called SUSY seesaw).

Supersymmetric seesaws lead to a number of possible signatures in the neutral and charged lepton sectors, both at low and high energies. Among low-energy observables, the most striking SUSY seesaw impact is perhaps the possibility of having charged lepton flavour violating (LFV) transitions. Indeed, one can have sizable contributions to radiative decays ( $\ell_i \rightarrow \ell_j \gamma$ ), three-body decays ( $\ell_i \rightarrow 3\ell_j$ ) and  $\mu - e$  transitions in heavy nuclei, well within reach of current and/or future dedicated facilities [7–29]. At high-energy colliders, such as the LHC, several observables may reflect an underlying SUSY seesaw. Let us begin by noticing that if some components of the seesaw mediators are not singlets under the SM gauge group (which is the case in type II and III seesaws), the latter can leave an imprint on the SUSY spectrum, since they can modify the supersymmetric  $\beta$ -functions governing the evolution of the gauge couplings and soft-SUSY breaking parameters. At the LHC, SUSY seesaws can also give rise to several LFV signals: firstly, one can have sizable widths for LFV decay processes like  $\chi_2^0 \rightarrow \chi_1^0 \ell_i^\pm \ell_j^\mp$  [27, 30–33]; secondly, one can have observable flavoured slepton mass splittings (MS),  $\Delta m_{\tilde{\ell}}/m_{\tilde{\ell}}$  ( $\tilde{e}_L, \tilde{\mu}_L$ ) and  $\Delta m_{\tilde{\ell}}/m_{\tilde{\ell}}$  ( $\tilde{\mu}_L, \tilde{\tau}_2$ ). These splittings can be identified since, under certain conditions, one can effectively reconstruct slepton masses via observables such as the kinematic end-point of the invariant mass distribution of the leptons coming from the cascade decays  $\chi_2^0 \rightarrow \tilde{\ell}^\pm \ell^\mp \rightarrow \chi_1^0 \ell^\pm \ell^\mp$ . If the slepton in the decay chain is real (on-shell), the di-lepton invariant mass spectrum has a kinematical edge that might then be measured with a very high precision (up to 0.1 %) [34–36]. Together with data arising from other observables, this information allows to reconstruct the slepton masses [34–38] and hence study the slepton mass splittings. Finally, one can observe multiple edges in di-lepton invariant mass distributions from  $\chi_2^0 \rightarrow \chi_1^0 \ell_i^\pm \ell_i^\mp$ , arising from the exchange of a different flavour slepton  $\tilde{\ell}_j$  (in addition to the left- and right-handed sleptons,  $\tilde{\ell}_{L,R}^i$ ). Under the assumption of a seesaw as the unique underlying source of flavour violation in the leptonic sector (for instance assuming that SUSY breaking is due to flavour blind interactions), then all the above observables, both at high and low energies, will be strongly correlated.

Each seesaw realisation will have a distinct impact on the latter observables. It is thus manda-

tory to conduct an exhaustive study of the many possible experimental signatures, in order to test the seesaw hypothesis, either excluding or substantiating it, and in the latter case, devising a strategy to disentangle among the different seesaw realisations.

In a previous work [39] we have studied the impact of a type I seesaw, embedded into the constrained minimal supersymmetric extension of the SM (cMSSM), in what concerns lepton flavour violation both at low-energies and at the LHC. Here we extend the analysis to the type III SUSY seesaw. In this case, and in order to accommodate neutrino masses and mixings, one adds (at least two) fermionic SU(2) triplets to the SM particle field content [40], as well as the corresponding superpartners. If one extends the usual MSSM by just the superfields responsible for neutrino masses and mixings, one would destroy the nice feature of gauge coupling unification. This problem is easily circumvented by embedding the new states in complete SU(5) representations, **24**-plets in the case of a type III seesaw [41]. Note that in addition to the SU(2) triplet, the **24**-plet contains a singlet state which also contributes to neutrino dynamics, so that in this case one actually has a mixture between type I and type III seesaws.

Our study shows that if a type III seesaw is indeed the unique source of neutrino masses and leptonic mixings, and is realised within an otherwise flavour conserving SUSY extension of the SM (specifically the cMSSM), one then expects low-energy LFV observables within future sensitivity reach, as well as interesting slepton phenomena at the LHC. After having identified regions in the cMSSM parameter space, where the slepton masses could in principle be reconstructed from the kinematical edges of di-lepton mass distributions (i.e.  $\chi_2^0 \rightarrow \chi_1^0 \ell_i^\pm \ell_i^\mp$  can occur, and with a non-negligible number of events), we study the different slepton mass splittings, exploring the implications for LFV decays. From the comparison of the predictions for the two sets of observables (high- and low-energy) with the current experimental bounds and future sensitivities, one can either derive information about the otherwise unreachable seesaw parameters, or disfavour the type III SUSY seesaw as being the unique source of lepton flavour violation.

The paper is organised as follows: in Section 2 we define the model, providing a brief overview on the implementation of a type III seesaw in the cMSSM. In Section 3 we discuss the implications of this mechanism for low- and high-energy LFV observables. Our results are presented in Section 4 where we study the different high- and low-energy observables in the seesaw case. This will also allow to draw some conclusions on the viability of a supersymmetric type III seesaw as the underlying mechanism of LFV. Further discussion is presented in the concluding Section 5.

## 2 Type III SUSY seesaw

Under the hypothesis that neutrinos are Majorana particles, the smallness of their masses, as well as their mixings, can be explained via seesaw-like mechanisms due to the exchange of heavy states: fermionic singlets (type I), scalar triplets (type II) or fermionic triplets (type III). The three possible seesaw realisations can be easily embedded in the framework of supersymmetric models. However, if SUSY's appealing feature of gauge coupling (and gaugino mass) unification is to be preserved, the new particles present below the Grand Unified scale must belong to complete GUT representations. Under the assumption of an SU(5) gauge group, generating a neutrino mass matrix with at least two non-zero eigenvalues<sup>1</sup> requires the following multiplet content: two copies of **1** or **24** (type I and III, respectively) or  $\overline{\mathbf{15}} + \mathbf{15}$  (type II). The addition of the non-singlet fields (i.e. the **15**- and the **24**-plets) has an important effect on the evolution of several fundamental parameters, especially on the  $\beta$ -functions for gauge and Yukawa couplings, as well as on the

---

<sup>1</sup>Rank  $\geq 2$  neutrino mass matrices can also be obtained with a truly minimal heavy field content, via the inclusion of non-renormalisable operators in the superpotential (see, for example, [42, 43]).

Renormalisation Group (RG) running of mass-terms above the seesaw scale. At low-energies (electroweak scale) this translates into changes in the SUSY spectrum, leading to scenarios that can be significantly different from a minimal supergravity (mSUGRA) inspired (or minimal type I SUSY seesaw) scenario. In turn, this will have consequences concerning flavour observables and cosmological quantities like the dark matter relic density.

We consider in this study a generic framework where three families of triplet fermions,  $\Sigma_i$  (as well as their superpartners) are added to the MSSM particle content [44]. Each one is embedded into a **24**-plet<sup>2</sup>, that decomposes under the SM gauge group,  $SU(3) \times SU(2) \times U(1)$ , as

$$\begin{aligned} \mathbf{24} &= (8, 1, 0) + (3, 2, -5/6) + (3^*, 2, 5/6) + (1, 3, 0) + (1, 1, 0) \\ &= \widehat{G}_M + \widehat{X}_M + \widehat{\bar{X}}_M + \widehat{W}_M + \widehat{B}_M. \end{aligned} \quad (2.1)$$

The fermionic components of the last two terms in the above decomposition ( $\widehat{W}_M$  and  $\widehat{B}_M$ ) have exactly the same quantum numbers of a fermionic triplet ( $\Sigma$ ) and of a singlet right-handed neutrino ( $\nu_R$ ). It is then clear that if embedded into an  $SU(5)$  framework, the realisation of the type III seesaw will in general produce a mixture of type I and type III mechanisms.

In the unbroken  $SU(5)$  phase, the superpotential is given by

$$\mathcal{W}^{SU(5)} = \sqrt{2} \bar{\mathbf{5}}_{M_i} Y_{ij}^5 \mathbf{10}_{M_j} \bar{\mathbf{5}}_H - \frac{1}{4} \mathbf{10}_{M_i} Y_{ij}^{10} \mathbf{10}_{M_j} \mathbf{5}_H + \mathbf{5}_H \mathbf{24}_{M_i} Y_{ij}^N \bar{\mathbf{5}}_{M_j} + \frac{1}{4} \mathbf{24}_{M_i} M_{24ij} \mathbf{24}_{M_j}, \quad (2.2)$$

with  $i, j$  denoting generation (flavour) indices, and where we have not included the terms specifying the Higgs sector responsible for the breaking of  $SU(5)$ . The Majorana mass term in Eq. (2.2) is gauge invariant due to having the triplet superfields in the adjoint  $SU(2)$  representation. In the broken phase, in addition to the usual MSSM terms, the superpotential is given by:

$$\begin{aligned} \mathcal{W} &= \mathcal{W}^{\text{MSSM}} + \widehat{H}_2 \left( \widehat{W}_M Y_M - \sqrt{\frac{3}{10}} \widehat{B}_M Y_B \right) \widehat{L} + \widehat{H}_2 \widehat{\bar{X}}_M Y_X \widehat{D}^c + \\ &+ \frac{1}{2} \widehat{B}_M M_B \widehat{B}_M + \frac{1}{2} \widehat{G}_M M_G \widehat{G}_M + \frac{1}{2} \widehat{W}_M M_W \widehat{W}_M + \widehat{X}_M M_X \widehat{\bar{X}}_M. \end{aligned} \quad (2.3)$$

After the heavy fields are integrated out, and at lowest order in the expansion in  $(v_2 Y_{B,W}/M_{B,W})^n$  ( $v_2$  being the vacuum expectation value of  $H_2^0$ ), one obtains the light neutrino mass matrix:

$$m_\nu \approx -v_2^2 \left( \frac{3}{10} Y_B^T M_B^{-1} Y_B + \frac{1}{2} Y_W^T M_W^{-1} Y_W \right), \quad (2.4)$$

where we have again omitted flavour indices. From the above formula, it is clear that we are indeed in the presence of a mixed type I and III seesaw, with contributions to  $m_\nu$  arising from both the singlets ( $\propto Y_B$ ) and  $SU(2)$  triplets ( $\propto Y_W$ ). The model is further specified by  $\mathcal{W}^{\text{MSSM}}$  and by the soft-SUSY breaking Lagrangian. Concerning the latter, we will furthermore assume a cMSSM framework, where mSUGRA-inspired universality conditions for the soft-breaking SUSY parameters are imposed at some very high-energy scale, which we take to be  $M_{\text{GUT}}$ . The MSSM part of the model is then defined by the usual 4 continuous parameters (the universal gaugino and scalar soft-breaking masses  $M_{1/2}$  and  $m_0$ , the universal trilinear coupling  $A_0$  and the ratio of the Higgs vacuum expectation values,  $\tan \beta = v_2/v_1$ ) and the sign of the bilinear  $\mu$ -term in  $\mathcal{W}^{\text{MSSM}}$ ,  $\text{sign}(\mu)$ .

---

<sup>2</sup>Among the representations of lower dimension, only the **24** does indeed contain a singlet hypercharge field.

One can further impose additional GUT scale SU(5)-motivated boundary conditions for the Yukawa couplings and Majorana masses appearing in Eq. (2.3):  $Y_B = Y_W = Y_X$  and  $M_B = M_W = M_G = M_X$ . Although the above parameters do run between the GUT scale and their corresponding decoupling scales, one has, to a very good approximation, that  $Y_B \simeq Y_W$  and  $M_B \simeq M_W$  as the heavy states decouple. At the seesaw scale (which we define to be  $\approx M_B \simeq M_W$ )  $m_\nu$  is approximately given by

$$m_\nu \approx -v_2^2 \frac{4}{5} Y^{\nu T} M_N^{-1} Y^\nu, \quad (2.5)$$

where we have again used the simplifying notation  $Y_B = Y_W = Y_N = Y^\nu$ ,  $M_B = M_W = M_N$ .

Up to an overall factor (4/5), one can still use the Casas-Ibarra parametrization [12] for the neutrino Yukawa couplings at the seesaw scale  $M_N$ ,

$$Y^\nu v_2 = i \sqrt{M_N^{\text{diag}}} R \sqrt{m_\nu^{\text{diag}}} U_{\text{MNS}}^\dagger. \quad (2.6)$$

In the above  $R$  is a complex orthogonal  $3 \times 3$  matrix that encodes the possible mixings involving the heavy neutral states, in addition to those of the low-energy sector (i.e.  $U_{\text{MNS}}$ ), and which is parametrized in terms of three complex angles  $\theta_i$  ( $i = 1, 2, 3$ ).

As extensively discussed in [44], the  $\beta$ -functions of the gauge couplings, as well as the running for soft gaugino and scalar masses, are strongly affected in type III seesaw models. In fact, RGE effects are behind the relatively small interval for  $M_N$  in a type III SUSY seesaw. Assuming that the triplet masses are degenerate ( $M_{N_i} = M_{24}$ ), the interval is bounded from above,  $M_{24} \lesssim 9 \times 10^{14}$  GeV, to comply with the atmospheric neutrino mass difference. On the other hand, for triplet masses below  $10^{13}$  GeV, the running is such that one encounters Landau poles for the gauge couplings at the GUT scale, while tachyonic sfermions (especially the lighter stau and stop) can also arise for smaller values of the soft-SUSY breaking parameters.

As clear from the above discussion, the new distinctive features of a type III seesaw will likely be manifest in many phenomena. In what follows we discuss the new contributions of the type III SUSY seesaw for low-energy lepton flavour violation (e.g. to radiative decays such as  $\mu \rightarrow e\gamma$ ), as well as for LFV at the LHC: in particular, we focus on the study of slepton mass splittings to probe deviations from the cMSSM and possibly derive information about the SUSY seesaw parameters.

### 3 Lepton flavour violation in a type III SUSY seesaw

As for the case of a type I SUSY seesaw, the non-trivial flavour structure of  $Y^\nu$  at the GUT scale will induce (through the running from  $M_{\text{GUT}}$  down to the seesaw scale) flavour mixing in the otherwise approximately flavour conserving soft-SUSY breaking terms. In particular, there will be radiatively induced flavour mixing in the slepton mass matrices, manifest in the  $LL$  and  $LR$  blocks of the  $6 \times 6$  slepton mass matrix; an analytical estimation using the leading order (LLog) approximation leads to the following corrections to the slepton mass terms [44]:

$$\begin{aligned} (\Delta m_L^2)_{ij} &= -\frac{9}{5} \frac{1}{8\pi^2} (3m_0^2 + A_0^2) (Y^{\nu\dagger} L Y^\nu)_{ij}, \\ (\Delta A_l)_{ij} &= -\frac{9}{5} \frac{3}{16\pi^2} A_0 Y_{ij}^l (Y^{\nu\dagger} L Y^\nu)_{ij}, \\ (\Delta m_E^2)_{ij} &\simeq 0; L_{kl} \equiv \log \left( \frac{M_X}{M_{N_k}} \right) \delta_{kl}. \end{aligned} \quad (3.1)$$

When compared to the type I SUSY seesaw, the most important difference corresponds to a change in the overall factor (multiplying the  $(Y^{\nu\dagger} L Y^\nu)_{ij}$  term). The above sources of flavour mixing will have an impact regarding lepton flavour non-universality and lepton flavour violation in the charged slepton sector, potentially inducing sizable contributions to high- and low-energy LFV observables, as we proceed to discuss.

As mentioned in the Introduction, several LFV signals can be observable at the LHC, in strict relation with the  $\chi_2^0 \rightarrow \chi_1^0 \ell^\pm \ell^\mp$  decay chains. As discussed in [34–38], in scenarios where the  $\chi_2^0$  is sufficiently heavy to decay via a real (on-shell) slepton, the process  $\chi_2^0 \rightarrow \chi_1^0 \ell^\pm \ell^\mp$  is greatly enhanced while providing a very distinctive signal: same-flavour opposite-charged leptons with missing energy. The  $\chi_2^0 \rightarrow \chi_1^0 \ell^\pm \ell^\mp$  decay chain thus offers a golden laboratory to study LFV at the LHC, via the following observables:

- (i) sizable widths for LFV decay processes like  $\chi_2^0 \rightarrow \chi_1^0 \ell_i^\pm \ell_j^\mp$  [27, 30–33];
- (ii) multiple edges in di-lepton invariant mass distributions  $\chi_2^0 \rightarrow \chi_1^0 \ell_i^\pm \ell_i^\mp$ , arising from the exchange of a different flavour slepton  $\tilde{\ell}_j$  (in addition to the left- and right-handed sleptons,  $\tilde{\ell}_{L,R}^i$ );
- (iii) flavoured slepton mass splittings.

In order to optimise the reconstruction of the leptons’ momentum (which is expected to be easy, accounting for smearing effects in  $\tau$ ’s) and, in addition, extract indirect information on the mass spectrum of the involved sparticles, the SUSY spectrum must comply with the requirements of a so-called “standard window”:

- (a) the spectrum is such that the decay chain  $\chi_2^0 \rightarrow \tilde{\ell} \ell \rightarrow \chi_1^0 \ell \ell$ , with intermediate real sleptons, is allowed;
- (b) it is possible to have sufficiently hard outgoing leptons:  $m_{\chi_2^0} - m_{\tilde{\ell}_L, \tilde{\tau}_2} > 10 \text{ GeV}$ .

In this case, the di-lepton invariant mass spectrum has a kinematical edge that might be measured with a very high precision (up to 0.1 %) [34–36]. Together with data arising from other observables, this information allows to reconstruct the slepton masses [34–38], and hence probe slepton mass universality or test LFV in the slepton sector. In particular, the relative slepton mass splittings, which are defined as

$$\frac{\Delta m_{\tilde{\ell}}(\tilde{\ell}_i, \tilde{\ell}_j)}{m_{\tilde{\ell}}} = \frac{|m_{\tilde{\ell}_i} - m_{\tilde{\ell}_j}|}{\langle m_{\tilde{\ell}_{i,j}} \rangle}, \quad (3.2)$$

can be inferred from the kinematical edges with a sensitivity of  $\mathcal{O}(0.1\%)$  [45] for  $\tilde{e}_L - \tilde{\mu}_L$  and  $\mathcal{O}(1\%)$  for  $\tilde{\mu}_L - \tilde{\tau}_2$ .

Even in the absence of a seesaw mechanism, it is important to recall that universality between the third and first two slepton generations is broken due to  $LR$  mixing and to RGE effects proportional to the third generation lepton Yukawa coupling. However, in the presence of flavour violation (as induced by the SUSY seesaw, see Eqs. (3.1)), the mass differences between left-handed selectrons, smuons and staus can be potentially augmented. Similar to the case of a type I seesaw [39], the relative mass splitting between left-handed sleptons is approximately given by

$$\frac{\Delta m_{\tilde{\ell}}(\tilde{\ell}_i, \tilde{\ell}_j)}{m_{\tilde{\ell}}} \approx \frac{|(\Delta m_L^2)_{ij}|}{m_\ell^2} \quad (3.3)$$

where we have neglected  $LR$  mixing effects, as well as RGE contributions proportional to the charged lepton Yukawa coupling. In the  $R = 1$  seesaw limit, where all flavour violation in  $Y^\nu$  stems from the  $U_{\text{MNS}}$  (see Eq. (2.6)), and assuming that the large flavour violating entries involving the second and third generation constitute the dominant source of mixing (and are thus at the



origin of the slepton mass differences), one can further relate the  $\tilde{e}_L - \tilde{\mu}_L$  and the  $\tilde{\mu}_L - \tilde{\tau}_2$  mass differences [39]:

$$\frac{\Delta m_{\tilde{\ell}}}{m_{\tilde{\ell}}}(\tilde{e}_L, \tilde{\mu}_L) \approx \frac{1}{2} \frac{\Delta m_{\tilde{\ell}}}{m_{\tilde{\ell}}}(\tilde{\mu}_L, \tilde{\tau}_2). \quad (3.4)$$

As discussed in [39], in the framework of a type I seesaw, the slepton mass differences can be sufficiently large as to be within the reach of LHC sensitivity.

Before proceeding, let us briefly notice that, depending on the amount of flavour violation, one can be led to regimes where two non-degenerate mass eigenstates have almost identical flavour content (maximal flavour mixing). To correctly interpret a mass splitting between sleptons with quasi-degenerate flavour content, one has to introduce an “effective” mass

$$m_i^{(\text{eff})} \equiv \sum_{X=\tilde{\tau}_2, \tilde{\mu}_L, \tilde{e}_L} m_{\tilde{l}_X} \left( |R_{X i_L}^{\tilde{l}}|^2 + |R_{X i_R}^{\tilde{l}}|^2 \right), \quad (3.5)$$

where  $R^{\tilde{l}}$  is the matrix that diagonalizes the  $6 \times 6$  slepton mass matrix. The effective mass splittings are then defined as

$$\left( \frac{\Delta m}{m} \right)^{(\text{eff})}(\tilde{\ell}_i, \tilde{\ell}_j) \equiv \frac{2 |m_i^{(\text{eff})} - m_j^{(\text{eff})}|}{m_i^{(\text{eff})} + m_j^{(\text{eff})}}. \quad (3.6)$$

The seesaw-generated flavour violating entries of Eqs. (3.1) will also give rise to low-energy LFV phenomena, such as radiative  $\ell_i \rightarrow \ell_j \gamma$  decays, which are induced by 1-loop diagrams via the exchange of gauginos and sleptons. These can be described by the effective Lagrangian [7],

$$\mathcal{L}_{\text{eff}} = e \frac{m_{\ell_i}}{2} \bar{\ell}_i \sigma_{\mu\nu} F^{\mu\nu} (A_L^{ij} P_L + A_R^{ij} P_R) \ell_j + \text{h.c.}, \quad (3.7)$$

where  $P_{L,R} = \frac{1}{2}(1 \mp \gamma_5)$  are the usual chirality projectors and the couplings  $A_L$  and  $A_R$  arise from loops involving left- and right-handed sleptons, respectively. Using Eq. (3.7), the branching ratio  $\ell_i \rightarrow \ell_j \gamma$  is given by

$$\text{BR}(\ell_i \rightarrow \ell_j \gamma) = \frac{48\pi^3 \alpha}{G_F^2} \left( |A_L^{ij}|^2 + |A_R^{ij}|^2 \right) \text{BR}(\ell_i \rightarrow \ell_j \nu_i \bar{\nu}_j). \quad (3.8)$$

where  $G_F$  is the Fermi constant and  $\alpha$  is the electromagnetic coupling constant. In our numerical calculation we use the exact expressions for  $A_L$  and  $A_R$ <sup>3</sup>. However, for an easier understanding of the numerical results, we note that the relations between these couplings and the slepton soft-breaking masses are approximately given by

$$|A_L^{ij}| \sim \frac{|(\Delta m_L^2)_{ij}| \tan \beta}{m_{\text{SUSY}}^4} \simeq \left| \frac{9}{5} \frac{\tan \beta}{8\pi^2} \frac{(3m_0^2 + A_0^2)}{m_{\text{SUSY}}^4} (Y^{\nu\dagger} L Y^\nu)_{ij} \right|, \quad A_R^{ij} \sim \frac{(\Delta m_E^2)_{ij} \tan \beta}{m_{\text{SUSY}}^4} \simeq 0, \quad (3.9)$$

where  $m_{\text{SUSY}}$  denotes a generic (average) SUSY mass and where we have used Eqs. (3.1).

It is important to notice here that when compared to other seesaws, and for the same cMSSM parameters, the sparticle spectrum is lighter. Together with the larger Yukawa couplings (a consequence of the larger seesaw scale), the type III seesaw typically leads to larger LFV observables than in either type I or II [44].

---

<sup>3</sup>The exact formulae for the branching ratios of the radiative LFV decays, as used in our numerical computation, can be found, for example, in [46].

Equally interesting LFV observables are  $\mu - e$  conversions in heavy nuclei, as they offer challenging experimental prospects: the possibility of improving experimental sensitivities to values as low as  $\sim 10^{-18}$  renders this observable an extremely powerful probe of LFV in the muon-electron sector. In the limit of photon-penguin dominance, the conversion rate  $\text{CR}(\mu - e, N)$  and  $\text{BR}(\mu \rightarrow e\gamma)$  are strongly correlated, since both observables are sensitive to the same leptonic mixing parameters [28].

In the following section we numerically analyse the above discussed points.

## 4 Numerical results and discussion

For the numerical computation, we have used the public code SPHENO (v3.beta.51) [47] to carry out the numerical integration of the RGEs. The RGEs of the SU(5) type III SUSY seesaw were calculated at 2-loop level in [44], using the public code SARAH [48]. SPHENO further computes the sparticle and Higgs spectrum, as well as the various low-energy LFV observables. The dark matter relic density is evaluated through a link to MICROMEGAS v2.2 [49].

Regarding low-energy neutrino data, current (best-fit) analyses favour the following intervals for the mixing angles [50]

$$\theta_{12} = (34.4 \pm 1.0)^\circ, \quad \theta_{23} = (42.8^{+4.7}_{-2.9})^\circ, \quad \theta_{13} = (5.6^{+3.0}_{-2.7})^\circ (\leq 12.5^\circ), \quad (4.1)$$

while for the mass-squared differences one has

$$\Delta m_{21}^2 = (7.6 \pm 0.2) \times 10^{-5} \text{ eV}^2, \quad \Delta m_{31}^2 = \begin{cases} (-2.36 \pm 0.11) \times 10^{-3} \text{ eV}^2 \\ (+2.46 \pm 0.12) \times 10^{-3} \text{ eV}^2 \end{cases}, \quad (4.2)$$

where the two ranges for  $\Delta m_{31}^2$  correspond to inverted and normal neutrino spectrum. In Table 1 we summarise the current bounds and the future sensitivities of dedicated experimental facilities, for the low-energy LFV observables considered in our numerical discussion.

LFV process	Present bound	Future sensitivity
$\text{BR}(\mu \rightarrow e\gamma)$	$1.2 \times 10^{-11}$ [51]	$10^{-13}$ [52]
$\text{BR}(\tau \rightarrow \mu\gamma)$	$4.5 \times 10^{-8}$ [53]	$10^{-9}$ [54]
$\text{CR}(\mu - e, \text{Ti})$	$4.3 \times 10^{-12}$ [51]	$\mathcal{O}(10^{-16})$ ( $\mathcal{O}(10^{-18})$ ) [55] ( [56])

Table 1: Present bounds and future sensitivities for several LFV observables.

In the first part of the analysis we assume a degenerate spectrum for the three families of triplet fermions. Moreover, we consider the conservative limit<sup>4</sup> in which flavour violation solely arises from the  $U_{\text{MNS}}$  leptonic mixing matrix, i.e.  $R = 1$  in Eq. (2.6). Leading to the results displayed in this section, we have taken into account all available LEP and Tevatron bounds on the Higgs boson and SUSY spectrum [51, 57, 58], as well as the most recent results on negative SUSY searches from the LHC collaborations [59, 60].

---

<sup>4</sup>In general, the limit  $R = 1$  translates into a “conservative” limit for flavour violation: apart from possible cancellations, and for a fixed seesaw scale, this limit typically provides a lower bound for the amount of generated LFV.



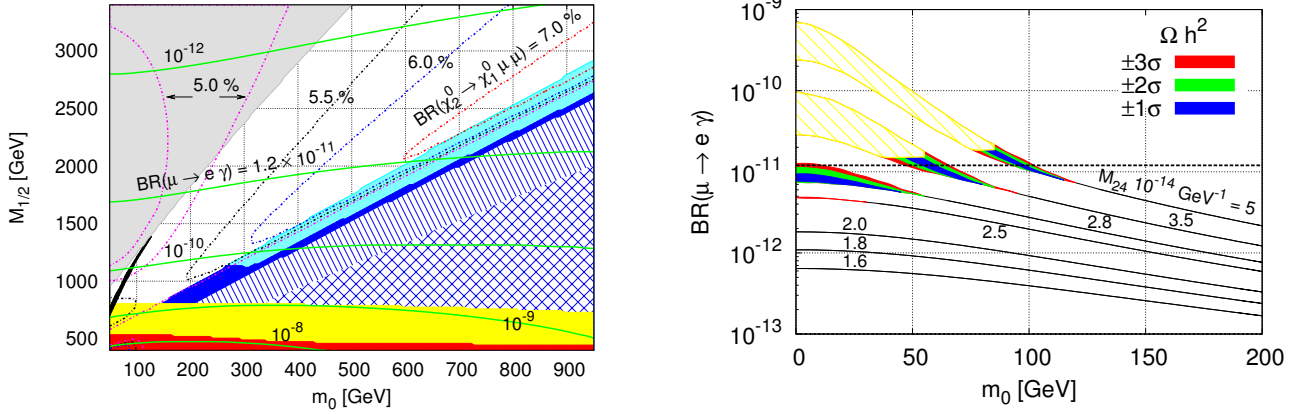


Figure 1: On the left,  $m_0 - M_{1/2}$  plane (in GeV), with  $A_0 = 0$ ,  $\tan \beta = 10$ , for a seesaw scale  $M_{24} \sim 5 \times 10^{14}$  GeV and  $\theta_{13} = 0.1^\circ$ . The shaded region on the left is excluded due to the presence of a charged LSP, while the yellow (red) region is excluded in view of  $m_{h_1^0}$  bounds ( $m_{h_1^0}$  and LHC bounds). Several regions do not fulfil the “standard window” requirements: solid regions correspond to having  $m_{\chi_2^0} < m_{\tilde{\ell}_L} + 10$  GeV (cyan) and  $m_{\chi_2^0} < m_{\tilde{\tau}_2} + 10$  GeV (blue). The dashed blue region corresponds to  $m_{\chi_2^0} < m_{\tilde{\ell}_L, \tilde{\tau}_2}$  while blue crosses correspond to  $m_{\chi_2^0} < m_{\tilde{\tau}_1} + m_\tau$ . The centre white region denotes the parameter space obeying the “standard window” constraint. Green lines denote isocurves for  $\text{BR}(\mu \rightarrow e \gamma)$ , while the dashed-dotted lines correspond to different values of  $\text{BR}(\chi_2^0 \rightarrow \chi_1^0 \mu \mu)$  as indicated in the plot. A small black region in the lower left corner corresponds to a WMAP7 compatible  $\chi_1^0$  relic density. On the right panel,  $\text{BR}(\mu \rightarrow e \gamma)$  as a function of  $m_0$  (in GeV), for  $A_0 = 0$ ,  $\tan \beta = 5$ ,  $\theta_{13} = 0.1^\circ$  and several values of  $M_{24}$ :  $1.6 \times 10^{14}$  GeV  $\lesssim M_{24} \lesssim 5 \times 10^{14}$  GeV (from lower to upper curves). Horizontal lines correspond to the current bound and future sensitivity. The yellow gridded region is excluded due to violation of  $m_{h_1^0}$  bounds. The colour code denotes compatibility with the WMAP7 bounds on  $\Omega h^2$ .

Concerning the WMAP7 bound for the observed dark matter relic density [6],

$$0.0941 \lesssim \Omega h^2 \lesssim 0.1277, \quad (4.3)$$

we do not systematically impose it as a viability requirement in our analysis. Nevertheless, we do require the lightest neutralino to be the lightest SUSY particle (LSP). We will return to this issue at a later stage.

Let us then begin our discussion by investigating how the requirements of a “standard window”, as well as compatibility with experimental bounds, constrain the type III SUSY seesaw parameter space in the case of degenerate fermion triplets (i.e.,  $M_{N_i} = M_{24}$ ).

On the left-hand side of Fig. 1, we display the  $m_0 - M_{1/2}$  parameter space for a type III SUSY seesaw, taking  $A_0 = 0$ ,  $\tan \beta = 10$ , and a seesaw scale  $M_{24} \sim 5 \times 10^{14}$  GeV, setting also  $\theta_{13} = 0.1^\circ$ . The excluded (shaded) areas correspond to a charged LSP, to the violation of collider constraints on the Higgs and sparticle spectrum, and to kinematically disfavoured regimes (kinematically closed  $\chi_2^0 \rightarrow \tilde{\ell} \ell$  channel, excessively soft outgoing leptons, etc.). The requirements of a “standard window” (see section 3) are fulfilled on the central white region. For this choice of SUSY seesaw parameters, a large part of the latter viable region is excluded since it is associated

with an excessively large  $\mu \rightarrow e\gamma$  branching ratio, as can be verified from the isocurves for the  $\text{BR}(\mu \rightarrow e\gamma)$ . Additional isocurves (dashed-dotted lines) denote  $\text{BR}(\chi_2^0 \rightarrow \chi_1^0 \mu\mu)$ . In the region complying with the “standard window” requirements, the latter range from 5% to 7%; for the LHC operating at  $\sqrt{s} = 7$  TeV, hardly any events would be observable, while for  $\sqrt{s} = 14$  TeV, one could expect some 10 to 1000 events (for an integrated luminosity of  $100 \text{ fb}^{-1}$ ). This implies that these  $\chi_2^0$  decay chains could indeed be studied at the higher luminosity and higher energy phase of LHC.

Concerning dark matter, it is important to notice that, although the requirements imposed on the  $\chi_2^0 \rightarrow \tilde{\ell}\ell$  decay usually lead to a region where the correct dark matter relic density could in principle be obtained from co-annihilations of the LSP with the next-to-LSP (NLSP), finding points for which  $\Omega h^2$  is indeed in agreement with WMAP7 data proves to be challenging. For the particular SUSY seesaw configuration investigated in Fig. 1, we verify that the regions where one finds the correct dark matter relic density are already excluded due to having an excessively large  $\text{BR}(\mu \rightarrow e\gamma)$ . Although viable DM scenarios in the type III SUSY seesaw are indeed very constrained [44], regions can be found where either by a different choice of seesaw parameters (e.g. setting  $\delta$ , the Dirac phase in  $U_{\text{MNS}}$ ,  $\delta = \pi$ ) or for smaller  $\tan\beta$  values, a viable  $\Omega h^2$  can be obtained, but still associated with a considerable fine tuning of the parameters. This is illustrated on the right-hand side plot of Fig. 1 for  $\tan\beta = 5$ , where we display  $\text{BR}(\mu \rightarrow e\gamma)$  as a function of  $m_0$  for several (7) choices of the seesaw scale,  $1.6 \times 10^{14} \text{ GeV} \lesssim M_{24} \lesssim 5 \times 10^{14} \text{ GeV}$ . When compatibility with the WMAP7  $3\sigma$  interval for  $\Omega h^2$  is indeed possible,  $M_{1/2}$  has been varied (corresponding to the coloured solid regions as well as the gridded ones - which are already excluded by collider constraints); else, we display the value of  $M_{1/2}$  that minimises the deviation from the WMAP7  $3\sigma$  interval (black curves). Typically, the correct relic density is obtained for nearly degenerate LSP and NLSP.

Contrary to the type I seesaw, where the requirements of observing the  $\chi_2^0 \rightarrow \chi_1^0 \ell\ell$  chain did not significantly alter the expected low-energy SUSY spectrum, important changes are expected in the type III seesaw, especially due to the (strong) running of the gaugino masses. Moreover, and as discussed previously, the allowed interval for the triplet masses ( $M_{24}$ ) is also severely constrained. To illustrate the impact of a “standard window” on the spectrum, we display in Fig. 2 the (geometrically) averaged squark masses as a function of the triplet mass, for different values of  $m_0$ . We consider two regimes of  $\tan\beta$ ,  $\tan\beta = 10, 40$ . For each point a scan over  $M_{1/2}$  is conducted to determine its lowest possible value complying with the requirement of a “standard window”. We also differentiate between the ranges allowed with and without applying the current bound on  $\text{BR}(\mu \rightarrow e\gamma)$ . Regarding mixings in the neutrino sector, we again work in the limit  $R = 1$  and set  $\theta_{13} = 0.1^\circ$ .

As can be seen from Fig. 2, and as hinted on section 2, the allowed interval for the seesaw scale (here represented by  $M_{24}$ ) ranges from  $10^{13} \text{ GeV}$  to just below  $10^{15} \text{ GeV}$ , corresponding to the results of [44]. It is worth emphasising that there are regions where, in addition to complying with all accelerator and neutrino data, the type III seesaw still leads to scenarios of LFV in agreement with low-energy data (the most stringent constraint arising from the  $\mu \rightarrow e\gamma$  decay). This diverges from the findings of [44], where only very light SUSY spectra were considered. Regimes of heavier sparticles (large  $M_{1/2}$  and  $m_0$ ) are preferred, confirming that these scenarios would be more likely to be observed at the LHC for  $\sqrt{s} = 14 \text{ TeV}$ . It is important to remark that, even for a regime of small  $m_0$ , we are always led to a very heavy SUSY spectrum (here represented by a geometrical average of the squark masses). Complying with all the above requirements implies that even for  $m_0$  as low as  $50 \text{ GeV}$ , one must have  $< m_{\tilde{q}} >^{\text{min}} \sim 2 \text{ TeV}$  (and around  $1.5 \text{ TeV}$  for the limiting case of  $m_0 = 0$ ). By itself, this result is important in the sense that should any light SUSY spectrum

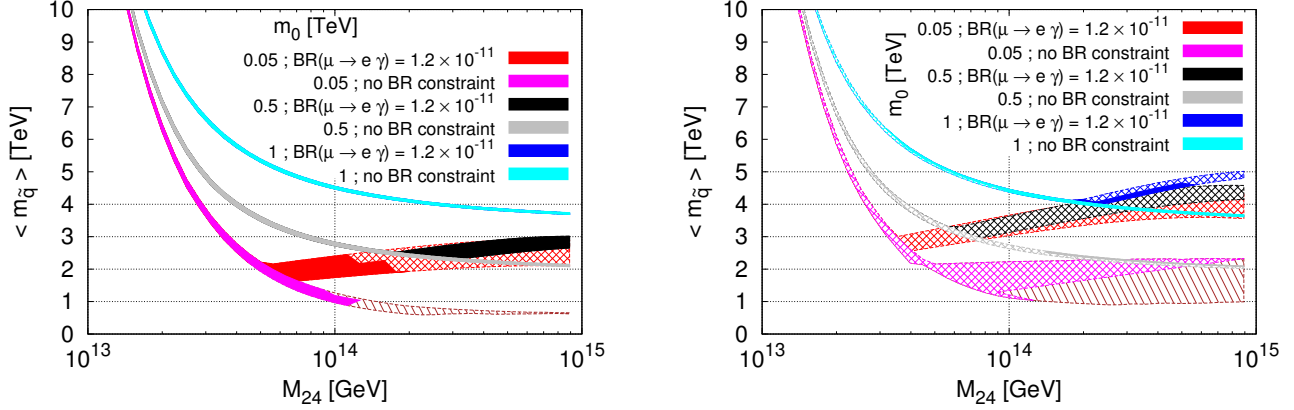


Figure 2: Average squark mass range (in TeV) as a function of the triplet mass (in GeV), for different values of  $m_0$ : 50 GeV (blue/cyan), 500 GeV (black/grey) and 1 TeV (red/pink), the colour code further denoting imposing/not imposing the bound on  $\text{BR}(\mu \rightarrow e\gamma)$ . Gridded regions correspond to cases where one has a charged LSP. The brown region is excluded due to violation of LHC or  $m_{h_1^0}$  bounds. The left (right) figure corresponds to  $\tan\beta = 10$  (40). In both cases,  $\theta_{13} = 0.1^\circ$ ,  $A_0 = \{-1, 0, 1\}$  TeV, with  $M_{1/2}$  set to the lowest possible value complying with the requirement of a “standard window”.

be discovered at the LHC in association with the  $\chi_2^0 \rightarrow \tilde{\ell}\ell$  decay chain, this would strongly suggest that a type III seesaw is not at work. It is also important to notice that the steep increase of  $\langle m_{\tilde{q}} \rangle$  for lower values of  $M_{24}$  is a direct consequence of having imposed the requirement of a “standard window”. In particular the strong running of  $M_2$  would imply that for lower  $M_{24}$  the mass of the sleptons would be much larger than that of the neutralinos, thus preventing the cascade decay  $\chi_2^0 \rightarrow \tilde{\ell}\ell$ .

Increasing the value of  $\tan\beta$  has an effect on the SUSY contributions to the LFV observables (which grow with  $\tan^2\beta$ , see Eq. (3.9)), implying that larger values of the SUSY spectrum (and hence of  $M_{1/2}$ ) are required to comply with the experimental constraints. Furthermore, the augmentation of the  $LR$  mixing in the stau sector implies that having a neutral LSP becomes increasingly difficult. For  $\tan\beta = 40$ , as depicted on the right-hand side of Fig. 2, the allowed regions are extremely reduced: only a thin blue band (corresponding to  $m_0 = 1$  TeV) survives all constraints. To further clarify and illustrate the above discussion regarding the dependence of the sparticle spectrum on the seesaw scale (under the requirements of a “standard window” and compatibility with experimental bounds), we present on Fig. 3 the electroweak gaugino and slepton masses as a function of the triplet mass ( $M_{24}$ ), also explicitly denoting the value of  $A_0$  in each case. Being essentially driven by  $M_{1/2}$ , the running of their values is similar to that of the (averaged) squark masses.

Finally, let us notice that variations of the still unknown Chooz angle,  $\theta_{13}$ , have a comparatively small impact: they only contribute to some of the LFV observables and compatibility with the experimental bound is easily recovered through a minor augmentation of  $M_{1/2}$ , which in turn leads to a heavier sparticle spectrum (for fixed values of  $m_0$ ).

We now focus our discussion on the slepton mass differences, as potentially measurable at the LHC. We recall that the expected (conservative) sensitivities for the slepton mass splittings are

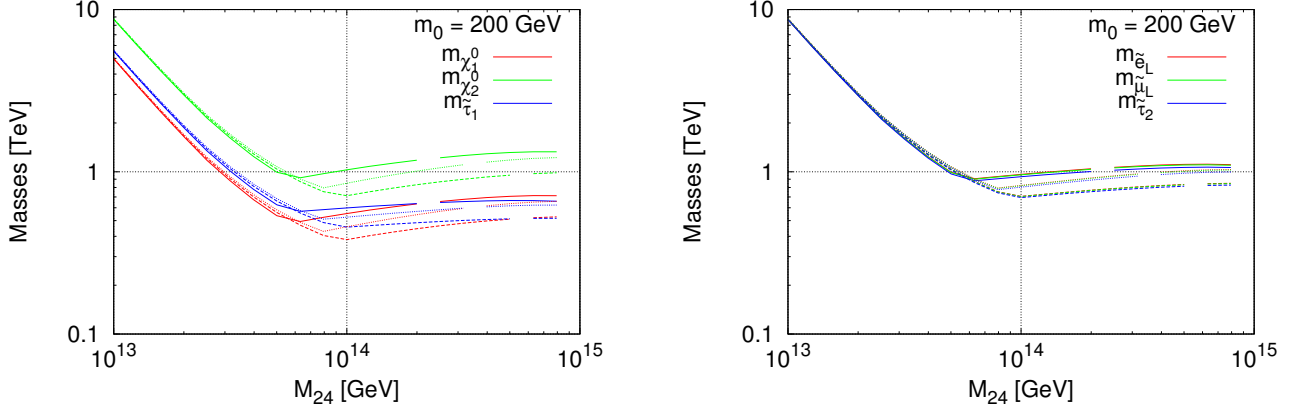


Figure 3: Gaugino and slepton masses (in TeV) as a function of the triplet mass,  $M_{24}$  (in GeV), for  $m_0 = 200$  GeV. On the left,  $m_{\chi_{1,2}^0}$  and  $m_{\tilde{\tau}_1}$ ; on the right  $m_{\tilde{e}_L}$ ,  $m_{\tilde{\mu}_L}$  and  $m_{\tilde{\tau}_2}$ . We have taken  $\tan\beta = 10$  and set  $\theta_{13} = 0.1^\circ$ .  $M_{1/2}$  is set to the lowest possible value complying with the requirement of a “standard window” and with the bound on  $\text{BR}(\mu \rightarrow e\gamma)$ . In both cases, the different lines correspond to distinct values of  $A_0$ : -1 TeV (full), 0 (dashed), and 1 TeV (dotted). An interrupted line signals the onset of a charged LSP region.

of  $\mathcal{O}(0.1\%)$  for  $\Delta m_{\tilde{e}}/m_{\tilde{e}}$  ( $\tilde{e}, \tilde{\mu}$ ) and  $\mathcal{O}(1\%)$  for  $\Delta m_{\tilde{e}}/m_{\tilde{e}}$  ( $\tilde{\mu}, \tilde{\tau}$ ). In Figs. 4 we display the slepton mass splittings (effective mass difference in the case of  $\tilde{e}_L - \tilde{\mu}_L$ ) as a function of the seesaw scale, for the same parameter scan as in Figs. 2. One verifies that  $\Delta m_{\tilde{e}}/m_{\tilde{e}}$  ( $\tilde{e}_L, \tilde{\mu}_L$ ) can be as large as 3% and  $\Delta m_{\tilde{e}}/m_{\tilde{e}}$  ( $\tilde{\mu}_L, \tilde{\tau}_2$ )  $\sim 5\%$ , for the maximal values of the seesaw scale, and for large  $m_0$  regimes (where the largest amount of flavour violation, still compatible with experimental bounds and with the requirements of a “standard window”, occurs). For larger values of  $\tan\beta$ , one could have slightly larger  $\tilde{\mu}_L - \tilde{\tau}_2$  mass splittings (mostly in association with larger  $LR$  mixings in the stau sector), but the viable regions in the parameter space are much smaller, as mentioned before. In all cases one always has  $\Delta m_{\tilde{e}}/m_{\tilde{e}}$  ( $\tilde{\mu}_L, \tilde{\tau}_2$ )  $\lesssim 7\%$ .

When compared to a type I SUSY seesaw (see [39]), one realises that the maximal values of the slepton mass splittings are slightly smaller, which is a consequence of the somewhat heavier SUSY spectrum. Concerning the mass splittings of right-handed sleptons, and analogous to the type I case, one finds a very small effect: in fact, for the parameter space surveyed in Fig. 4 (and always under the imposition of a “standard window” as well as compatibility with collider constraints),  $\Delta m_{\tilde{e}}/m_{\tilde{e}}$  ( $\tilde{\mu}_R, \tilde{e}_R$ )  $\lesssim 0.1\%$ .

Finally, assuming that slepton mass differences are measured close to their maximal values ( $\sim 3\%$  for  $\tilde{\mu}_L - \tilde{e}_L$  and  $\sim 5\%$  for  $\tilde{\mu}_L - \tilde{\tau}_2$ ) and that the reconstructed value of  $m_0$  is found to be large (around 1 TeV) then, as seen from Figs. 4, this would suggest that the seesaw scale would be  $M_{24} \sim 10^{15}$  GeV (for the limiting case  $R = 1$ ).

In Fig. 5 we present the comparison of the  $\tilde{e}_L - \tilde{\mu}_L$  and  $\tilde{\mu}_L - \tilde{\tau}_2$  mass differences, as well as their ratio, as a function of the seesaw scale. Similar to what occurs for a type I SUSY seesaw, and as discussed in Section 3, the mass differences are strongly correlated (being driven by the  $(\Delta m_L^2)_{23}$  entry in the slepton mass matrix). With the exception of the regions corresponding to smaller values of  $M_{24}$ , the relation  $\Delta m_{\tilde{e}}/m_{\tilde{e}}$  ( $\tilde{e}_L, \tilde{\mu}_L$ )  $\approx \mathcal{O}(1/2)\Delta m_{\tilde{e}}/m_{\tilde{e}}$  ( $\tilde{\mu}_L, \tilde{\tau}_2$ ) (Eq. (3.4)) typically holds to a very good approximation (with corrections due to fact that flavour conserving radiative corrections driven by the tau Yukawa coupling now play a non-negligible rôle). For lower

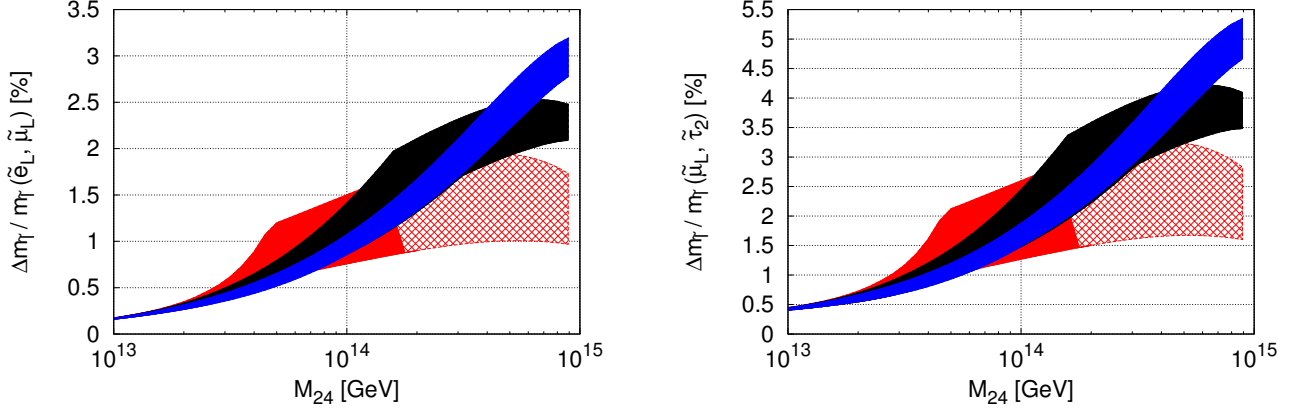


Figure 4: On the left,  $\tilde{e}_L - \tilde{\mu}_L$  mass difference (normalised to an average slepton mass) as a function of the triplet mass,  $M_{24}$  (in GeV). On the right,  $\tilde{\mu}_L - \tilde{\tau}_2$  effective mass difference (normalised to the corresponding average slepton mass) also as a function of the seesaw scale. In both cases we take  $\tan \beta = 10$ ,  $\theta_{13} = 0.1^\circ$ , and consider different values of  $m_0$ : 50 GeV (red), 500 GeV (black), and 1 TeV (blue). Gridded regions correspond to a charged LSP. For each point one varies  $A_0 = \{-1, 0, 1\}$  TeV, while  $M_{1/2}$  is set to the lowest possible value complying with the requirement of a “standard window” and with the bound on  $\text{BR}(\mu \rightarrow e\gamma)$ .

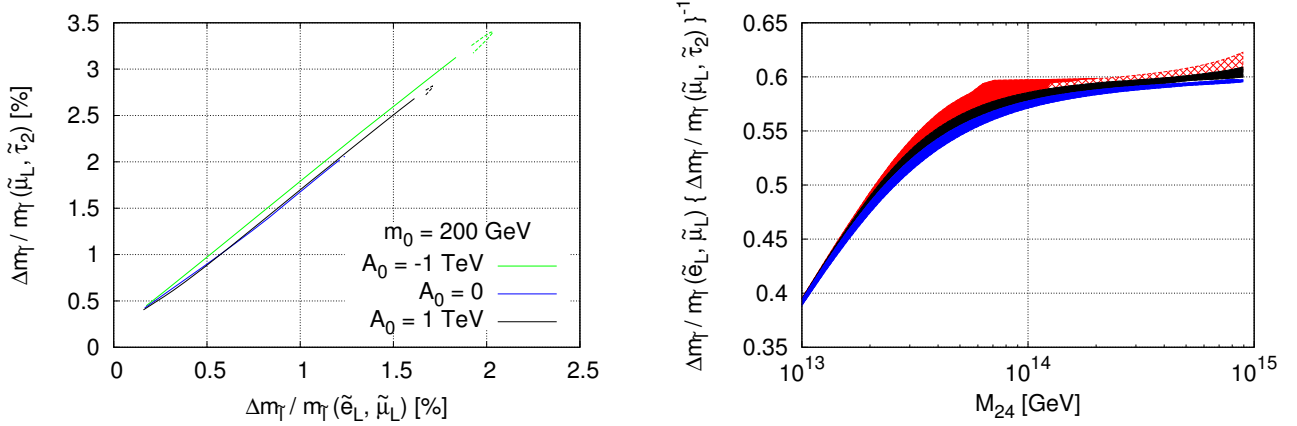


Figure 5: On the left,  $\Delta m_{\tilde{\ell}}/m_{\tilde{\ell}} (\tilde{\mu}_L, \tilde{\tau}_2)$  as a function of  $\Delta m_{\tilde{\ell}}/m_{\tilde{\ell}} (\tilde{e}_L, \tilde{\mu}_L)$ , for  $m_0 = 200$  GeV,  $\tan \beta = 10$ ,  $\theta_{13} = 0.1^\circ$  and taking  $A_0 = \{-1, 0, 1\}$  TeV (green, blue and black lines, respectively). An interrupted (dashed) line signals the onset of a charged LSP regime towards larger values of the mass splittings. On the right, ratio of slepton mass differences,  $\Delta m_{\tilde{\ell}} (\tilde{e}_L, \tilde{\mu}_L) / \Delta m_{\tilde{\ell}} (\tilde{\mu}_L, \tilde{\tau}_2)$  (normalised to the corresponding average slepton mass), as a function of the triplet mass (in GeV), for different values of  $m_0$ , with  $\tan \beta = 10$ ,  $A_0 = \{-1, 0, 1\}$  TeV and  $\theta_{13} = 0.1^\circ$ . Scan and colour code as in Fig. 4.

values of the seesaw scale, where the requirement of a “standard window” (i.e.  $\chi_2^0 \rightarrow \tilde{\ell}\ell$  decay, with hard outgoing leptons) forces a rapid increase of  $M_{1/2}$ , a small deviation to this strict correlation

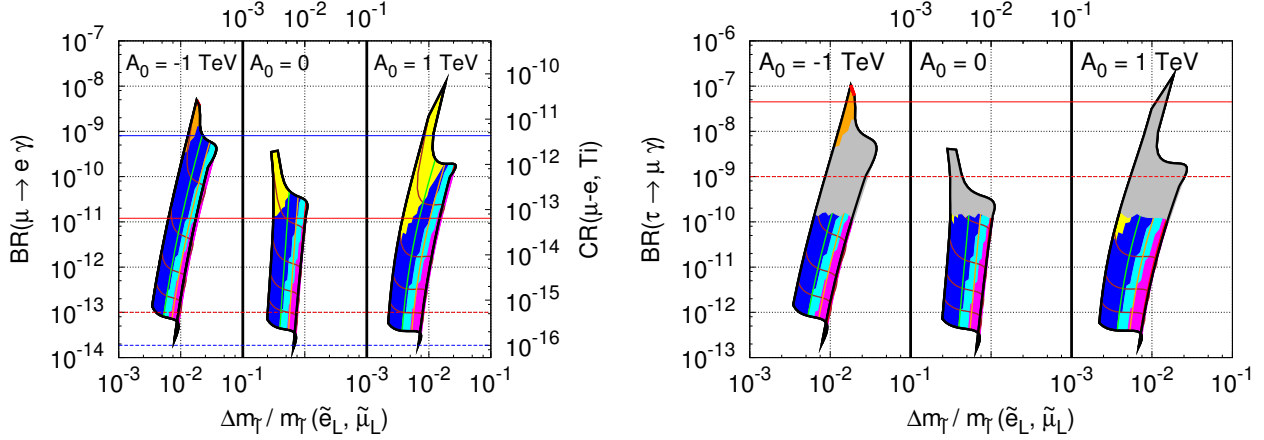


Figure 6:  $\text{BR}(\mu \rightarrow e\gamma)$  and  $\text{BR}(\tau \rightarrow \mu\gamma)$  as a function of the  $\tilde{e}_L - \tilde{\mu}_L$  slepton mass difference (normalised to an average slepton mass), corresponding to the left- and right-hand side panels. In both cases we have set  $m_0 = 100$  GeV,  $\tan\beta = 10$  and  $\theta_{13} = 0.1^\circ$ , and considered different values of the triplet scale  $M_{24}$  and of  $M_{1/2}$ . Each sub-panel corresponds to a distinct choice of  $A_0$ . Cyan regions correspond to fulfilling the requirements of a “standard window”. The bounds on  $m_{h_1^0}$  are violated in the yellow regions, LHC bounds on SUSY spectrum are violated in orange regions, while red regions are excluded due to both. Further excluded regions are due to failing to meet the kinematical constraints (blue), having a charged LSP (magenta) or violating another LFV bound (grey). Inset into each plot are “horizontal” isolines for  $M_{1/2}$  (ranging from 1.5 TeV to 6 TeV, from top to bottom) and “vertical” isolines for  $M_{24}$ : from left to right,  $10^{13}$  GeV to  $9 \times 10^{14}$  GeV. The secondary y-axis on the left-hand panel illustrates the corresponding values of  $\text{CR}(\mu - e, \text{Ti})$ . Horizontal lines denote the current experimental bounds (full) and future sensitivities (dashed).

is observed. This can also be seen in the left-hand side of Fig. 5, zooming into the lower end of the lines. We have verified that this behaviour occurs irrespective of the value of  $\theta_{13}$  and for all  $\tan\beta$  regimes (provided that the regions are phenomenologically and experimentally viable).

The correlation of low- and high-energy LFV observables is explored in Fig. 6, where we present  $\text{BR}(\mu \rightarrow e\gamma)$  and  $\text{BR}(\tau \rightarrow \mu\gamma)$  as a function of the  $\tilde{e}_L - \tilde{\mu}_L$  slepton mass difference, taking  $m_0 = 100$  GeV, and considering different values of the triplet scale,  $M_{24}$ . We also provide additional information about the  $\text{CR}(\mu - e, \text{Ti})$ . As seen from both panels of Fig. 6, only a small region of the scanned parameter space complies with the requirements of a “standard window” while being in agreement with the several experimental and phenomenological constraints. Similar to what occurs for a type I SUSY seesaw, larger, negative values of  $A_0$  translate into larger mass splittings. The maximal amount of flavour violation, both regarding radiative decays and slepton mass splittings, is obtained for: (i) a seesaw scale as large as possible (without violating perturbativity arguments, specifically on  $Y^\nu$ ), as can be understood from Eqs. (2.6, 3.1); (ii) lower values of  $M_{1/2}$  (leading to a lighter SUSY spectrum, see Eq. (3.9)). Regarding the  $\tau \rightarrow \mu\gamma$  decays, as can be seen from the right panel of Fig. 6, the regions in parameter space associated with  $\text{BR}(\tau \rightarrow \mu\gamma)$  within the sensitivity of SuperB are in fact excluded by the present bounds on  $\mu \rightarrow e\gamma$  decays. Although we do not present the corresponding results, a similar study with  $m_0 = 1$  TeV leads to scenarios of somewhat larger mass splittings, and smaller branching ratios for the radiative decays (due to the much heavier spectrum). It is nevertheless interesting to remark



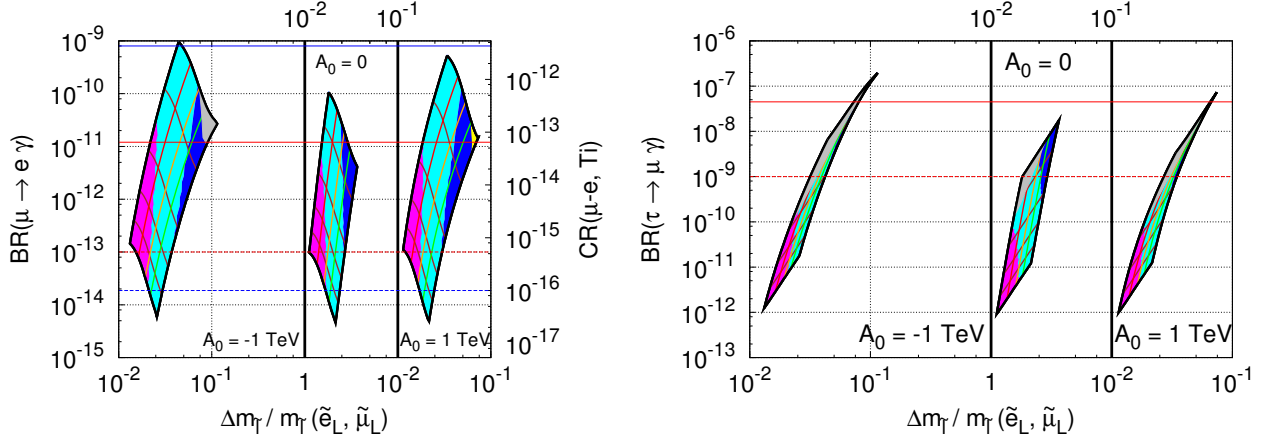


Figure 7: Non-degenerate triplet masses:  $\text{BR}(\mu \rightarrow e\gamma)$  and  $\text{BR}(\tau \rightarrow \mu\gamma)$  as a function of the  $\tilde{e}_L - \tilde{\mu}_L$  slepton mass difference (normalised to an average slepton mass), corresponding to the left- and right-hand side panels. Same scan as leading to Fig. 6, except that now  $M_{N_{1,3}}$  are fixed, with varying  $M_{N_2}$ :  $M_{N_1} = 10^{13} \text{ GeV} \lesssim M_{N_2} \lesssim 9 \times 10^{14} \text{ GeV} = M_{N_3}$ . Same line and colour code as in Fig. 6, the only exception being that the inset “vertical” isolines for  $M_{N_2}$  decrease from left to right.

that in this regime of very large  $m_0$ , one can have maximal mixings in the lightest slepton - now a composition of  $\tilde{\tau}_L$ ,  $\tilde{\tau}_R$  and  $\tilde{\mu}_L$  - possibly leading to scenarios of very large mass splittings (albeit for a tiny fraction of the parameter space).

Assuming that a type III seesaw is indeed the only source of LFV, and given the extremely constrained parameter space, one finds that in the conservative case of  $R = 1$ , the corresponding slepton mass splittings will always lie around the % level, and are thus within the expected sensitivity of the LHC. Furthermore, these mass splittings correspond to values of  $\text{BR}(\mu \rightarrow e\gamma)$  well within the expected sensitivity of MEG (or even already ruled out by current searches). Moreover, the regions lying below MEG sensitivity have an associated  $\text{CR}(\mu - e, \text{Ti})$  within the reach of future experiments (PRISM/PRIME).

We now consider more general scenarios of non-degenerate spectrum for the heavy triplets. In order to investigate this regime, we fix the heaviest (lightest) triplet mass to the upper (lower) limits of the  $M_{24}$  interval previously obtained, and allow the next-to-lightest triplet mass to vary between the latter limits. For such a non-degenerate triplet spectrum, we display in Fig. 7 an analogous study to that of Fig. 6 (same choice of the SUSY parameters, still working in the limiting case of  $R = 1$ ). As can be observed, the area complying with all requirements (cyan band) is now comparatively larger. The  $\tilde{e}_L - \tilde{\mu}_L$  slepton mass differences are also enhanced when compared to the degenerate case: for all three regimes of  $A_0 = -1, 0, 1 \text{ TeV}$ , one has  $1\% \lesssim \Delta m_{\tilde{e}}/m_{\tilde{e}}(\tilde{e}_L, \tilde{\mu}_L) \lesssim 10\%$ . Remarkably, one can have  $\Delta m_{\tilde{e}}/m_{\tilde{e}}(\tilde{e}_L, \tilde{\mu}_L) \sim 5\%$ , in agreement with current bounds on  $\text{BR}(\mu \rightarrow e\gamma)$ . Concerning the amount of LFV inducing the  $\mu \rightarrow e\gamma$  transitions, one finds that, similar to what occurs in the degenerate case, the largest BRs are associated with  $M_{N_2}$  close to its maximal allowed value (i.e.  $\sim M_{N_3}$ , leading to degenerate heavy and next-to-heavy triplets) and minimal values of  $M_{1/2}$ . While the latter leads to a lighter spectrum, the former allows to enhance the  $(Y^{\nu\dagger}LY^\nu)_{21}$  contributions proportional to  $M_{N_2}$ , which

are not suppressed by the smallness of  $\theta_{13}$ . However, it is important to notice that the same does not occur regarding  $\text{BR}(\tau \rightarrow \mu\gamma)$ , which is maximal for both minimal values of  $M_{1/2}$  and  $M_{N_2}$  (now degenerate with the lightest triplet). For fixed values of  $M_{N_{1,3}}$ , while the flavour violating entries responsible for  $\mu \rightarrow e\gamma$  transitions and other decays involving the first lepton family (i.e.  $(\Delta m_L^2)_{12}$  and  $(\Delta m_L^2)_{13}$ ) increase with increasing  $M_{N_2}$ ,  $(\Delta m_L^2)_{23}$  - which induces  $\text{BR}(\tau \rightarrow \mu\gamma)$  - remains approximately constant: in fact it actually decreases by a small factor, since the contributions proportional to  $M_{N_2}$  have the opposite sign of those associated to  $M_{N_3}$ .

Finally, and to conclude our numerical study, we have considered deviations from the  $R = 1$  limit, i.e., allowing for additional mixings in the seesaw mediators. Non-vanishing angles  $\theta_i$  lead to larger  $Y_{ij}^\nu$ , with implications for LFV observables: as expected (and aside from eventual accidental cancelations), there is a large enhancement of the contributions to low-energy LFV observables, as well as an increase of the mass splittings. More concretely, this would displace the cyan regions in Figs. 6 and 7 towards larger values of  $\text{BR}(\mu \rightarrow e\gamma)$  - potentially excluded by current bounds - and towards slightly larger  $\tilde{e}_L - \tilde{\mu}_L$  mass differences. Notice that when compared to the type I SUSY seesaw, the effects of  $R \neq 1$  are somewhat less important, since due to the much narrower interval of the seesaw scale (which is also heavier), perturbativity of  $Y^\nu$  effectively constraints the values of  $\theta_i$ . Concerning the impact of these variations on the SUSY spectrum (RGE induced), we have verified that deviations from  $R = 1$  have no effect on the gaugino and squark spectra.

To summarise, let us re-emphasise that should the  $\chi_2^0 \rightarrow \chi_1^0 \ell\ell$  decay chain be reconstructed at the LHC, a type III SUSY seesaw will be manifest in both low- and high-energy LFV observables, which will lie within the sensitivity of present/future experimental facilities. In other words, finding regions in the type III SUSY seesaw parameter space where the  $\chi_2^0 \rightarrow \chi_1^0 \ell\ell$  is present, without observing neither  $\mu \rightarrow e\gamma$  transitions at MEG, nor  $\Delta m_{\tilde{\ell}}/m_{\tilde{\ell}}$  ( $\tilde{e}_L, \tilde{\mu}_L$ ) at the LHC, is almost impossible.

## 5 Conclusions

Although it is a very appealing hypothesis to explain the origin of neutrino masses and mixings, the seesaw mechanism is in general very hard to probe directly. When embedded into a larger framework (as for instance SUSY models), where new states are active between the seesaw scale and the electroweak one, the seesaw mechanism can give rise to many distinct signatures, depending on the nature of the mediators: scalar or fermionic (gauge singlets or triplets). In this study we considered a supersymmetric type III seesaw where, in order to preserve gauge coupling unification, the additional states are embedded into complete  $\text{SU}(5)$  representations. The many experimental constraints (LEP, LHC, low-energy experiments) strongly reduce the available parameter space of the model, so that one expects very characteristic signals (SUSY spectrum and charged LFV, both at low-energies and at the LHC), which offer the possibility of falsifying the model. Using the correlation between the different LFV observables (inherent from the assumption that the seesaw provides the only source of flavour violation in the model), we have focused our analysis on the interplay between low-energy radiative decays (e.g.  $\mu \rightarrow e\gamma$ ) and potential LFV signatures appearing in association with the  $\chi_2^0 \rightarrow \tilde{\ell}\ell$  cascade decays at the LHC, such as flavoured slepton mass splittings,  $\Delta m_{\tilde{\ell}}/m_{\tilde{\ell}}$  ( $\tilde{e}_L, \tilde{\mu}_L$ ).

Firstly, requiring that the spectrum allows for the reconstruction of slepton masses from the  $\chi_2^0$  cascade decay chains (and assuming a  $\chi_1^0$  LSP), the type III SUSY seesaw leads to scenarios where a heavy SUSY spectrum (e.g.  $m_{\tilde{q}} \sim 2$  TeV) is in general favoured. Although viable dark matter scenarios are in general very hard to accommodate in the type III seesaw, we have nevertheless

verified that one can still find small regions in the parameter space where the  $\chi_1^0$  has the correct relic density. Such scenarios typically arise in association with the low  $m_0$  regime. Concerning dark matter, it is important to recall that other candidates might be present and have a relic density in agreement with WMAP bounds, as could be the case for gravitinos. However, this issue clearly lies beyond the scope of the present work.

Assuming that a type III seesaw is indeed the only source of LFV, and given the extremely constrained parameter space, one finds that the corresponding slepton mass splittings will always lie around the % level, and are thus within the expected sensitivity of the LHC. A hierarchical fermionic triplet spectrum further boosts the expected mass splittings: one is led to a regime where, even in the conservative limit of  $R = 1$ , one has  $1\% \lesssim \Delta m_{\tilde{e}}/m_{\tilde{e}} (\tilde{e}_L, \tilde{\mu}_L) \lesssim 5\%$ , in agreement with current bounds on charged LFV. Furthermore, these mass splittings correspond to values of  $\text{BR}(\mu \rightarrow e\gamma)$  well within the expected sensitivity of MEG (or, in very limiting cases, within PRISM/PRIME sensitivity for  $\text{CR}(\mu - e, \text{Ti})$ ).

In the more general case of an increased mixing involving the triplet sector (i.e.  $R \neq 1$ ), there is an enhancement of the contributions to low-energy LFV observables, as well as a small increase in the slepton mass splittings, without further impact on the remaining SUSY spectrum.

Unlike what occurs for a type I SUSY seesaw, the very constrained range for the type III seesaw scale strongly tightens the predictions for LFV: the expected flavoured mass splittings are indeed well within the sensitivity range of the LHC, while at the same time low-energy scale LFV must unavoidably lie within the present and future sensitivity of either MEG or PRISM/PRIME (observation of a  $\tau \rightarrow \mu\gamma$  signal at SuperB will be much more challenging). If supersymmetry is discovered at the LHC, and a type III seesaw is at the origin of flavour mixing in the lepton sector, then this model can be easily falsified in the near future.

## 6 Acknowledgements

This work has been done partly under the ANR project CPV-LFV-LHC NT09-508531. The work of A. J. R. F. has been supported by *Fundação para a Ciência e a Tecnologia* through the fellowship SFRH/BD/64666/2009. A. J. R. F. and J. C. R. also acknowledge the financial support from the EU Network grant UNILHC PITN-GA-2009-237920 and from *Fundação para a Ciência e a Tecnologia* grants CFTP-FCT UNIT 777, CERN/FP/83503/2008 and PTDC/FIS/102120/2008.

## References

- [1] P. Minkowski, Phys. Lett. B **67** (1977) 421; M. Gell-Mann, P. Ramond and R. Slansky, in *Complex Spinors and Unified Theories* eds. P. Van. Nieuwenhuizen and D. Z. Freedman, *Supergravity* (North-Holland, Amsterdam, 1979), p.315 [Print-80-0576 (CERN)]; T. Yanagida, in *Proceedings of the Workshop on the Unified Theory and the Baryon Number in the Universe*, eds. O. Sawada and A. Sugamoto (KEK, Tsukuba, 1979), p.95; S. L. Glashow, in *Quarks and Leptons*, eds. M. Lévy *et al.* (Plenum Press, New York, 1980), p.687; R. N. Mohapatra and G. Senjanović, Phys. Rev. Lett. **44** (1980) 912.
- [2] R. Barbieri, D. V. Nanopolous, G. Morchio and F. Strocchi, Phys. Lett. B **90** (1980) 91; R. E. Marshak and R. N. Mohapatra, *Invited talk given at Orbis Scientiae, Coral Gables, Fla., Jan. 14-17, 1980*, VPI-HEP-80/02; T. P. Cheng and L. F. Li, Phys. Rev. D **22** (1980) 2860; M. Magg and C. Wetterich, Phys. Lett. B **94** (1980) 61; G. Lazarides, Q. Shafi and C.

- Wetterich, Nucl. Phys. B **181** (1981) 287; J. Schechter and J. W. F. Valle, Phys. Rev. D **22** (1980) 2227; R. N. Mohapatra and G. Senjanović, Phys. Rev. D **23** (1981) 165.
- [3] E. Ma, Phys. Rev. Lett. **81** (1998) 1171 [arXiv:hep-ph/9805219]; R. Foot, H. Lew, X. G. He and G. C. Joshi, Z. Phys. C **44** (1989) 441.
  - [4] G. Jungman, M. Kamionkowski and K. Griest, Phys. Rept. **267** (1996) 195 [arXiv:hep-ph/9506380].
  - [5] G. Bertone, D. Hooper and J. Silk, Phys. Rept. **405** (2005) 279 [arXiv:hep-ph/0404175].
  - [6] D. Larson *et al.*, arXiv:1001.4635 [astro-ph.CO].
  - [7] J. Hisano, T. Moroi, K. Tobe and M. Yamaguchi, Phys. Rev. D **53** (1996) 2442 [arXiv:hep-ph/9510309].
  - [8] J. Hisano, T. Moroi, K. Tobe, M. Yamaguchi and T. Yanagida, Phys. Lett. B **357** (1995) 579 [arXiv:hep-ph/9501407].
  - [9] J. Hisano and D. Nomura, Phys. Rev. D **59** (1999) 116005 [arXiv:hep-ph/9810479].
  - [10] W. Buchmuller, D. Delepine and F. Vissani, Phys. Lett. B **459** (1999) 171 [arXiv:hep-ph/9904219].
  - [11] Y. Kuno and Y. Okada, Rev. Mod. Phys. **73** (2001) 151 [arXiv:hep-ph/9909265].
  - [12] J. A. Casas and A. Ibarra, Nucl. Phys. B **618**, 171 (2001) [arXiv:hep-ph/0103065].
  - [13] S. Lavignac, I. Masina and C. A. Savoy, Phys. Lett. B **520** (2001) 269 [arXiv:hep-ph/0106245].
  - [14] X. J. Bi and Y. B. Dai, Phys. Rev. D **66** (2002) 076006 [arXiv:hep-ph/0112077].
  - [15] J. R. Ellis, J. Hisano, M. Raidal and Y. Shimizu, Phys. Rev. D **66** (2002) 115013 [arXiv:hep-ph/0206110].
  - [16] F. Deppisch, H. Pas, A. Redelbach, R. Ruckl and Y. Shimizu, Eur. Phys. J. C **28** (2003) 365 [arXiv:hep-ph/0206122].
  - [17] T. Fukuyama, T. Kikuchi and N. Okada, Phys. Rev. D **68** (2003) 033012 [arXiv:hep-ph/0304190].
  - [18] A. Brignole and A. Rossi, Nucl. Phys. B **701** (2004) 3 [arXiv:hep-ph/0404211].
  - [19] A. Masiero, S. K. Vempati and O. Vives, New J. Phys. **6** (2004) 202 [arXiv:hep-ph/0407325].
  - [20] T. Fukuyama, A. Ilakovac and T. Kikuchi, Eur. Phys. J. C **56** (2008) 125 [arXiv:hep-ph/0506295].
  - [21] S. T. Petcov, W. Rodejohann, T. Shindou and Y. Takanishi, Nucl. Phys. B **739** (2006) 208 [arXiv:hep-ph/0510404].
  - [22] E. Arganda and M. J. Herrero, Phys. Rev. D **73** (2006) 055003 [arXiv:hep-ph/0510405].
  - [23] F. Deppisch, H. Pas, A. Redelbach and R. Ruckl, Phys. Rev. D **73** (2006) 033004 [arXiv:hep-ph/0511062].

- [24] C. E. Yaguna, Int. J. Mod. Phys. A **21** (2006) 1283 [arXiv:hep-ph/0502014].
- [25] L. Calibbi, A. Faccia, A. Masiero and S. K. Vempati, Phys. Rev. D **74** (2006) 116002 [arXiv:hep-ph/0605139].
- [26] S. Antusch, E. Arganda, M. J. Herrero and A. M. Teixeira, JHEP **0611** (2006) 090 [arXiv:hep-ph/0607263].
- [27] M. Hirsch, J. W. F. Valle, W. Porod, J. C. Romao and A. Villanova del Moral, Phys. Rev. D **78** (2008) 013006 [arXiv:0804.4072].
- [28] E. Arganda, M. J. Herrero and A. M. Teixeira, JHEP **0710** (2007) 104 [arXiv:0707.2955].
- [29] E. Arganda, M. J. Herrero and J. Portoles, JHEP **0806** (2008) 079 [arXiv:0803.2039 [hep-ph]].
- [30] N. Arkani-Hamed, H. Cheng, J. L. Feng and L. J. Hall, Phys. Rev. Lett. **77** (1996) 1937 [arXiv:hep-ph/9603431].
- [31] I. Hinchliffe and F. E. Paige, Phys. Rev. D **63** (2001) 115006 [arXiv:hep-ph/0010086].
- [32] D. F. Carvalho, J. R. Ellis, M. E. Gomez, S. Lola and J. C. Romao, Phys. Lett. B **618** (2005) 162 [arXiv:hep-ph/0206148].
- [33] E. Carquin, J. Ellis, M. E. Gomez, S. Lola and J. Rodriguez-Quintero, JHEP **0905** (2009) 026 [arXiv:0812.4243].
- [34] F. E. Paige, *Determining SUSY particle masses at LHC, in the proceedings of 1996 DPF/DPB Summer Study on New Directions for High-Energy Physics (Snowmass 96)*, June 25-July 12, Snowmass, Colorado, U.S.A. (1996), arXiv:hep-ph/9609373.
- [35] I. Hinchliffe, F. E. Paige, M. D. Shapiro, J. Soderqvist and W. Yao, Phys. Rev. D **55** (1997) 5520 [arXiv:hep-ph/9610544].
- [36] H. Bachacou, I. Hinchliffe and F. E. Paige, Phys. Rev. D **62** (2000) 015009 [arXiv:hep-ph/9907518].
- [37] G. L. Bayatian et al [CMS Collaboration], J. Phys. G **34** (2007) 995.
- [38] W. W. Armstrong et al [ATLAS Collaboration], *ATLAS: Technical proposal for a general-purpose p p experiment at the Large Hadron Collider at CERN*, CERN-LHCC-94-43; G. Aad et al [The ATLAS Collaboration], *Expected Performance of the ATLAS Experiment - Detector, Trigger and Physics*, arXiv:0901.0512.
- [39] A. Abada, A. J. R. Figueiredo, J. C. Romao and A. M. Teixeira, JHEP **1010** (2010) 104 [arXiv:1007.4833 [hep-ph]].
- [40] R. Foot, H. Lew, X. G. He and G. C. Joshi, Z. Phys. C **44** (1989) 441.
- [41] M. R. Buckley and H. Murayama, Phys. Rev. Lett. **97** (2006) 231801 [arXiv:hep-ph/0606088].
- [42] B. Bajc and G. Senjanovic, JHEP **0708** (2007) 014 [arXiv:hep-ph/0612029].
- [43] C. Biggio and L. Calibbi, JHEP **1010** (2010) 037 [arXiv:1007.3750 [hep-ph]].

- [44] J. N. Esteves, J. C. Romao, M. Hirsch, F. Staub and W. Porod, Phys. Rev. D **83** (2011) 013003 [arXiv:1010.6000 [hep-ph]].
- [45] B. C. Allanach, J. P. Conlon and C. G. Lester, Phys. Rev. D **77** (2008) 076006 [arXiv:0801.3666 [hep-ph]].
- [46] M. Raidal *et al.*, Eur. Phys. J. C **57** (2008) 13 [arXiv:0801.1826 [hep-ph]] and references therein.
- [47] W. Porod, Comput. Phys. Commun. **153** (2003) 275 [arXiv:hep-ph/0301101].
- [48] F. Staub, Comput. Phys. Commun. **181** (2010) 1077-1086, arXiv:0806.0538 [hep-ph].
- [49] G. Belanger, F. Boudjema, A. Pukhov and A. Semenov, Comput. Phys. Commun. **180** (2009) 747 [arXiv:0803.2360 [hep-ph]].
- [50] M. C. Gonzalez-Garcia, M. Maltoni and J. Salvado, JHEP **1004** (2010) 056 [arXiv:1001.4524 [hep-ph]].
- [51] K. Nakamura *et al.* [Particle Data Group], J. Phys. G **37** (2010) 075021.
- [52] O. A. Kiselev [MEG Collaboration], Nucl. Instrum. Meth. A **604** (2009) 304.
- [53] K. Hayasaka *et al.* [Belle Collaboration], Phys. Lett. B **666** (2008) 16 [arXiv:0705.0650 [hep-ex]].
- [54] M. Bona *et al.*, arXiv:0709.0451 [hep-ex].
- [55] D. Glenzinski, AIP Conf. Proc. **1222** (2010) 383.
- [56] Y. G. Cui *et al.* [COMET Collaboration], *Conceptual design report for experimental search for lepton flavor violating  $\mu^- - e^-$  conversion at sensitivity of  $10^{-16}$  with a slow-extracted bunched proton beam (COMET)*, KEK-2009-10.
- [57] R. Barate *et al.* [LEP Working Group for Higgs boson searches and ALEPH and DELPHI and L3 and OPAL Collaborations], Phys. Lett. **B565** (2003) 61 [hep-ex/0306033].
- [58] See talks by P. Totaro and K. Petridis at the *XLVIth Rencontres de Moriond*, La Thuile, 13-20 March 2011.
- [59] G. Aad *et al.* [ATLAS Collaboration], arXiv:1102.2357 [hep-ex].
- [60] V. Khachatryan *et al.* [CMS Collaboration], Phys. Lett. **B698** (2011) 196 [arXiv:1101.1628 [hep-ex]].